

Ultrafast Plasmonic Control of Second Harmonic Generation

Roderick B. Davidson II,^{*,†,‡} Anna Yanchenko,^{†,¶} Jed I. Ziegler,[†] Sergey M. Avanesyan,[†] Ben J. Lawrie,[‡] and Richard F. Haglund Jr.[†]

Department of Physics and Astronomy, Vanderbilt University, Nashville, Tennessee 37235-1807, USA, Computational Sciences and Engineering Division, Oak Ridge National Laboratory, Oak Ridge, Tennessee 37831, USA, and Department of Physics, University of Virginia, Charlottesville, Virginia 22904-4714, USA

E-mail: roderick.b.davidson@vanderbilt.edu

Abstract

Efficient frequency modulation techniques are crucial to the development of plasmonic metasurfaces for information processing and energy conversion. Nanoscale field confinement in optically pumped plasmonic structures enables stronger nonlinear susceptibilities than are attainable in bulk materials. Exposing materials to plasmonically driven electric fields allows for all-optical modulation of nonlinear signals. Here we demonstrate efficient second harmonic generation (SHG) in a serrated nanogap plasmonic geometry that generates steep electric field gradients within a dielectric material. We utilize an ultrafast optical pump to control plasmonically induced electric-fields and to generate bandwidth-limited second-harmonic pulses.

^{*}To whom correspondence should be addressed

[†]Department of Physics and Astronomy, Vanderbilt University, Nashville, Tennessee 37235-1807, USA

[‡]Computational Sciences and Engineering Division, Oak Ridge National Laboratory, Oak Ridge, Tennessee 37831, USA

[¶]Department of Physics, University of Virginia, Charlottesville, Virginia 22904-4714, USA

All-optical control of these designer plasmonic metasurfaces enables ultrafast switching technologies for on-chip nonlinear processes.

The manipulation of nonlinear optical phenomena using plasmonic control and near-field enhancement has recently enabled new ways to create active nanoscale photonic elements.¹⁻³ Several plasmonic geometries have been used to investigate the effects of plasmonic field confinement and asymmetry in second-order nonlinear optical processes.⁴⁻⁸ Dielectric materials near the surface of plasmonic nanoparticles exhibit enhanced nonlinear optical responses proportional to the confinement of the electric field.^{9,10} Second-harmonic efficiencies as high as 10^{-4} have been reported for dielectric systems controlled by plasmonic metasurfaces that will enable a wide variety of ultrafast optical modulation techniques.^{11,12} The short excitation lifetime and nanoscale footprint of metasurface devices hold promise for replacing macroscopic nonlinear crystals in biophotonic applications and tunable light sources. While the efficiency of these metal-dielectric coupled systems continues to grow, controlling these systems at timescales that would utilize the ultrashort plasmonic lifetimes remains a pressing concern.

While active control over nonlinear plasmonic interactions has been achieved through direct electrical contact, these means defeat the principal advantages afforded by plasmonic systems, for instance, nanoscale footprints and femtosecond interaction times.^{13,14} While enabling ultrafast optical control over SHG in metal-dielectric nanocomposites, we also demonstrate a platform for the direct characterization of nanoscale dielectric materials exposed to electric fields oscillating at optical frequencies. Second-harmonic interferometric spectroscopy performed on metal-dielectric nanocomposite systems allows us to map the dynamics of plasmonic oscillations on a sub-femtosecond timescale.

The lithographically fabricated gold serrated nanogaps (SNG), shown in Fig.1, create a series of electric-field ‘hotspots’ in a planar capacitor-like geometry. When the nanostructure is excited by a control laser pulse with an 800 nm wavelength and 30 fs pulse duration polarized perpendicular to the gap, regions of high electric field form at the points of the teeth, creating steep electric field gradients within the nanogap. Fig. 1b shows finite-difference time-domain simulations of the

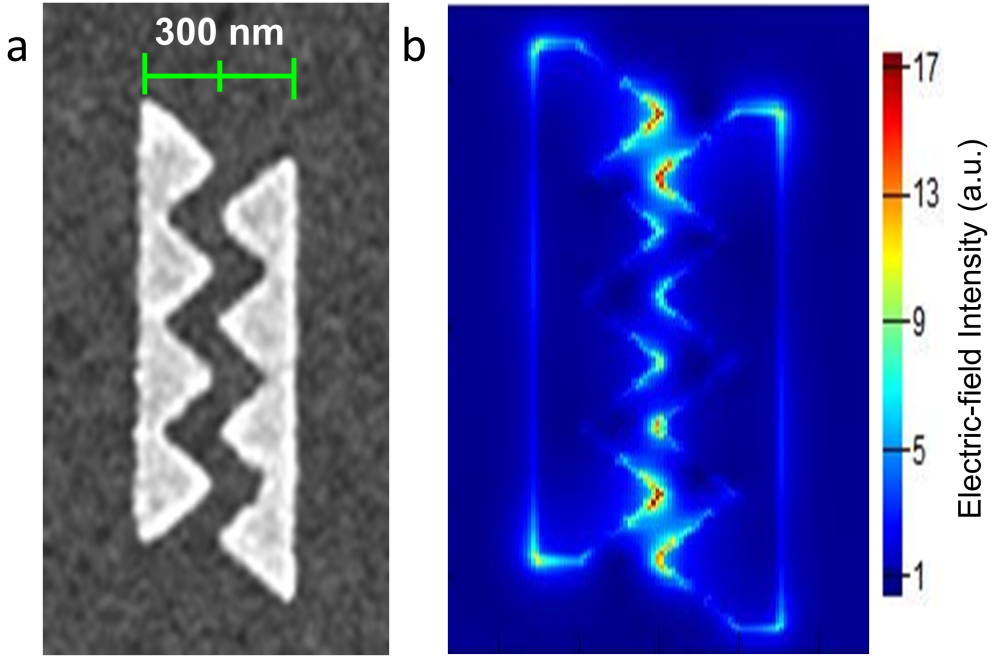


Figure 1: **The serrated nanogap.** **a**, SEM image of a SNG array. **b**, FDTD simulations of the near-field electric field intensity of the SNG plasmon excited with a pulse polarized perpendicular to the nanogap or horizontal to the image at $\lambda = 800\text{nm}$.

plasmonic evanescent electric field intensity generated by the control pulse. When the nanogap is filled by spin-coating poly(methyl methacrylate) (PMMA) onto the sample and the plasmon is excited using an ultrafast laser pulse, intense electric fields within the dielectric oscillate with a period of approximately 2.7 fs. These oscillations rapidly polarize the electronic structure of the PMMA, causing large changes in its effective second-order susceptibilities.

In order to demonstrate optical control over the SHG signal and isolate the SHG resulting from plasmonic modulation of the dielectric, we employ a spatial light modulator (SLM) as shown in Fig. 2a to generate a collinear orthogonally polarized pulse pair to simultaneously control and probe the plasmonic system. As shown in Fig. 2b, the control pulse polarized perpendicular to the

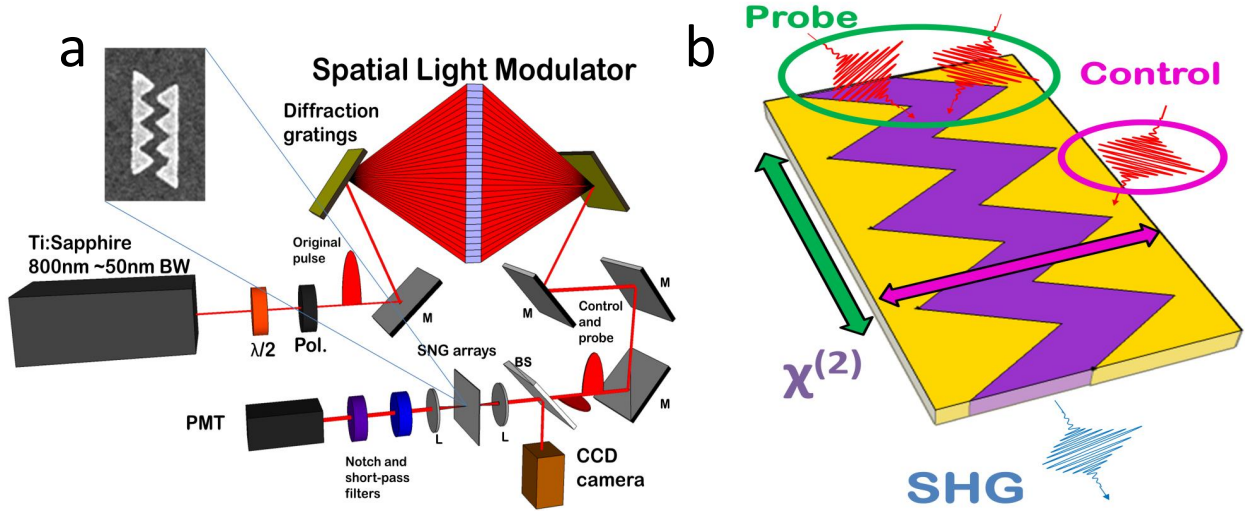


Figure 2: **Experimental set-up.** **a**, A Ti:Sapphire mode-locked laser is coupled with a spatial light modulator for temporal and polarization pulse control. The SLM generates transform limited control and probe pulses with orthogonal polarization and variable optical power and temporal delay from each 30 fs 800 nm pulse. **b**, The SNG structures are excited with a horizontally polarized control pulse (magenta) and probed with a vertically polarized probe pulse (green).

nanogap excites the plasmon, while the second pulse probes the state of the polarized dielectric. The orthogonally polarized pulses generate an interference pattern that is distinctive for structures with and without PMMA.

The SHG signal as a function of the relative temporal delay shows an interference between the control and the probe pulses as displayed in Fig. 3. Also, the high aspect ratio (4:1) of the SNG structure does not allow the probe pulse to be absorbed by the plasmon and thereby contribute to SHG due to plasmonic scattering. The interference peaks lie at $\tau=n\lambda/c$ delays and $\tau=n\lambda/2c$ delays. Peaks at $\tau=n\lambda/c$ correspond to the peak electric-field intensity of both the plasmon and laser pulse. Peaks at $\tau=n\lambda/2c$ lie where two 800 nm waves would normally destructively interfere and create an SHG minimum. This demonstrates that the interference pattern with two sets of maxima per oscillation, shown in Fig. 3a, is a result of the optical interaction with the plasmon driven polarization state of the dielectric. That is, were it not for the plasmonically induced interaction with the PMMA, interference maxima would appear only at $\tau=n\lambda/c$, because interference between two 800 nm pulses traveling through air would not experience this optical rectification.

To determine the conversion efficiency of the plasmon-enhanced SHG in PMMA, the same

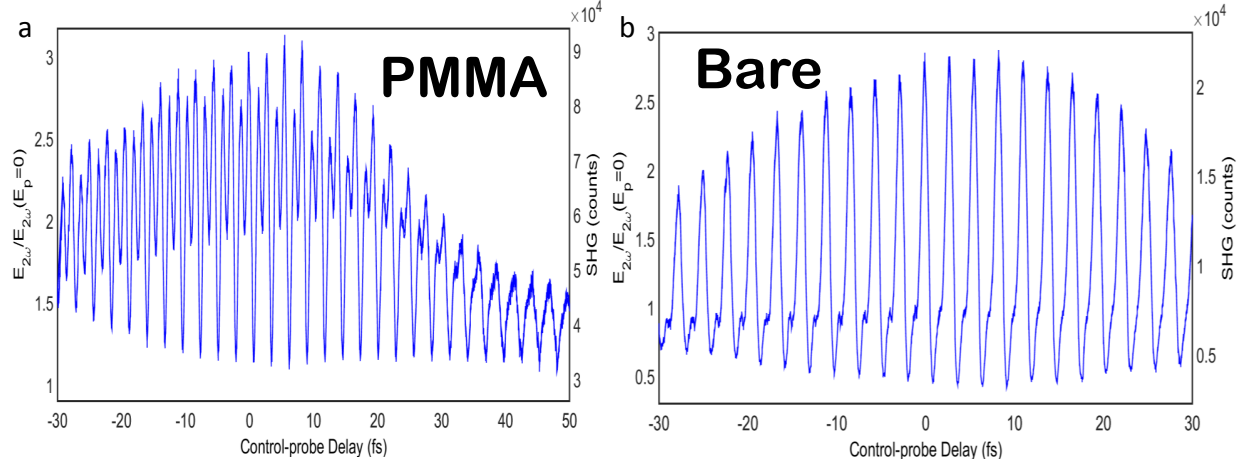


Figure 3: **Second-harmonic interference signal.** **a**, SHG as a function of control pulse-probe delay from a PMMA filled SNG. This measurement is normalized to the SHG signal from a horizontally polarized pulse. **b**, SHG from the same structure without the PMMA dielectric.

experiment was performed on a nanogap in the absence of PMMA. Fig. 3b shows the second-harmonic interference signal coming from the same lithographically fabricated structure as Fig. 3a before the deposition of the PMMA. Not only does the overall SHG conversion rate, referred to by the right hand axes, decrease four-fold, but the interference signature is that of a conventional optical interference pattern instead of the double-peaked pattern that appears with the PMMA dielectric. The interference pattern that remains is due to imperfect linear polarization of the pulse pairs generated in the SLM. There is also a small shoulder at the $\tau=n\lambda/2c$ delay points from plasmon-probe interference in the ITO/glass substrate. Since the evanescent field of the plasmon does not extend deep into the substrate, this signal is relatively small. A small change in the absorption of the plasmon due to the change in the dielectric environment after the PMMA removal can be seen in the supplementary information. However, the total change in the absorption was less than 5%, which is not sufficient to account for the change in SHG conversion efficiencies.

The left hand axes in both Figs. 3a and 3b show the SHG normalized to the signal from a control pulse in the absence of the probe. The overall switching contrast for the interference signal is 3:1 from peak to trough. The envelope of the SHG signal also shows that the second-harmonic pulse created by the plasmon-probe interaction has a duration less than 100fs. This is a result of the short duration of the plasmon excitation created by the transform-limited control pulse, which

has a pulse duration of 30 fs.

For time dependent external electric fields, the second-order polarizability depends on the second order susceptibility χ^2 as,

$$P_{2\omega}(E) \sim \chi^{(2)}(E_{\perp}) \int_0^{\tau_p} [E_{\parallel}(t+\tau)]^2 d\tau \quad (1)$$

Where E_{\parallel} represents the probe field amplitude from the pulse that is parallel to the gap, and E_{\perp} represents the electric field of the plasmon within the PMMA that is controlled by the pulse perpendicular to the gap.¹⁵ Since the PMMA dielectric is amorphous, it can utilize either of these fields for SHG conversion.

In order to determine the effect of the control pulse on the SHG conversion efficiency, the power of the control pulse was varied while holding the average power of the probe pulse at 10mW. Fig. 4a shows the change in the first optical cycle of interference after zero delay between the control and the probe pulse. Fig. 4b shows the height of the amplitude of the interference pattern as a function of the control pulse power. The curve fit indicates that $\chi^{(2)}$ depends on the square of the

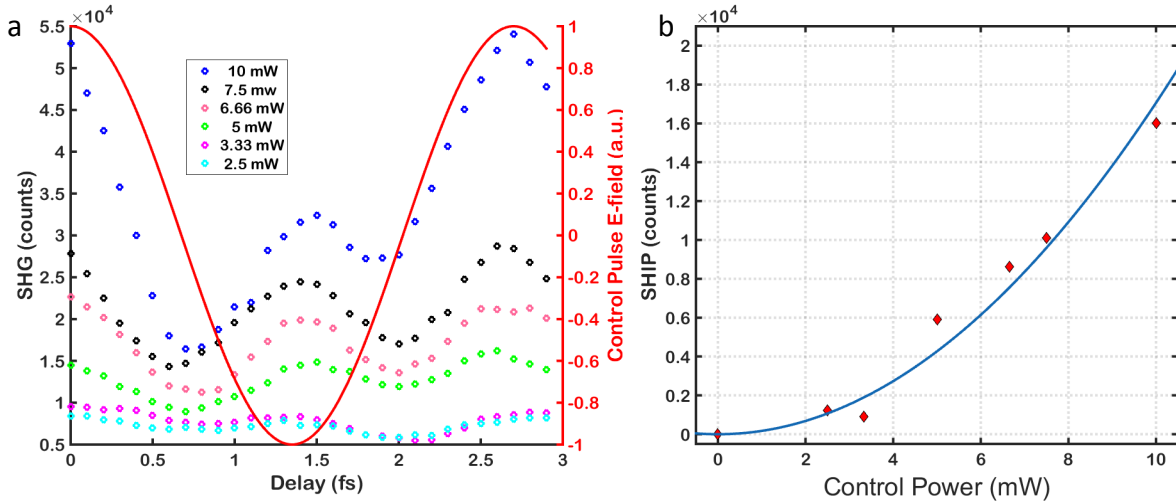


Figure 4: **Control Pulse-power dependence.** **a**, A single interference cycle of the SHG signal from a PMMA covered SNG for varying control pulse powers overlaid with the normalized electric field of the control pulse (red). **b**, Interference peak height from SHG maximum to minimum as a function of control pulse power. Measured interference heights are fitted to a quadratic function with no linear term with $R^2 = 0.98$.

control field for powers well below the optical damage threshold. A model describing this second order dependence will be the subject of future work involving highly nonlinear materials.

By demonstrating that the SHG efficiency for metamaterial controlled dielectrics scales quadratically with the control field, we have provided a robust platform for ultrafast switchable metasurfaces, efficiently generating nonlinear signals with pulse durations less than 100 fs. The SNG geometry can be used to study the optical properties of thin-film materials at nanometer length scales taking advantage of the polarizing effects of electric fields oscillating at optical frequencies. The interferometric spectroscopy enabled by the spatial light modulator makes it possible to separate plasmonically induced second-harmonic light within a dielectric material from light scattered by the plasmon. These experiments can be expanded to include materials with a larger χ^2 as well as materials with stronger polarizabilities such as ferroelectrics. This technique is not limited to second-order nonlinearities, which makes it possible to explore third-order nonlinear effects such as phase conjugation and absorption saturation on metasurfaces.

Materials and Methods

Output pulses from a mode-locked Ti:Sapphire laser oscillator were passed through and compressed by a SLM (Biophotonics Solutions Inc.) in order to achieve a transform limited pulse at the metasurface. The laser was pulsed at 83 MHz with a pulse width of 30 fs. This was focused onto the SNG array with a numerical aperture objective of 0.35. The SNGs were covered with 495PMMA A4 electron-beam resist. The resulting second-harmonic signals were detected using a Hamamatsu PMT (RU-9880U-110) connected to a Photon Counter (Stanford Research Systems).

The SLM consisted of 128 liquid crystal cells. Pulse pairs were generated by creating two phase masks from alternating liquid crystal cells to create identical spectral content.¹⁶ The phase mask was then altered for each measurement to scan the probe across the control field with a resolution of 100 μ m. In order to reduce the power of the control pulse, separate "dummy" pulses were created with a vertical polarization and temporal separation from the control of greater than 200 fs. These pulses did not contribute to the SHG signal, as confirmed by a hundred-fold

reduction in the SHG signal from a purely vertical excitation.

The dimensions of the SNG nanostructures required for resonant operation at 800 nm were calculated using Lumerical[®] FDTD software. The nanostructures were fabricated using standard electron-beam lithography and thermal evaporation of gold. A double-layer mask of PMMA 495A4 and 950A4 was used to optimize surface quality. All nanostructures were fabricated with a thickness of 40 nm.

Acknowledgement

RBD, SMA and JIZ were supported by the Office of Science, U.S. Department of Energy (DE-FG02-01ER45916). AY was supported by the National Science Foundation Research Experience for Undergraduates program of the Vanderbilt Institute of Nanoscale Science and Engineering (DMR-1263182). The nanogap samples were fabricated and characterized in facilities of the Vanderbilt Institute of Nanoscale Science and Engineering, which were renovated with funds provided by the National Science Foundation under the American Recovery and Reinvestment Act (ARI-R2 DMR-0963361). BJL and RBD acknowledge partial support from the Oak Ridge National Laboratory directed research and development program. Oak Ridge National Laboratory is operated by UT-Battelle for the U.S. Department of Energy under Contract No. DE-AC05-00OR22725.

References

- (1) Kauranen, M.; Zayats, A. V. Nonlinear plasmonics. *Nature Photonics* **2012**, *6*, 737–748.
- (2) Hess, O.; Pendry, J.; Maier, S.; Oulton, R.; Hamm, J.; Tsakmakidis, K. Active nanoplasmonic metamaterials. *Nature materials* **2012**, *11*, 573–584.
- (3) Melikyan, A.; Alloatti, L.; Muslija, A.; Hillerkuss, D.; Schindler, P.; Li, J.; Palmer, R.; Korn, D.; Muehlbrandt, S.; Van Thourhout, D. High-speed plasmonic phase modulators. *Nature Photonics* **2014**, *8*, 229–233.

(4) Davidson, R. B., II; Ziegler, J. I.; Vargas, G.; Avanesyan, S. M.; Haglund, R. F., Jr Efficient Forward Second-Harmonic Generation from Planar Archimedean Nanospirals. *Nanophotonics* **2015**, *4*, 108–113.

(5) Aouani, H.; Navarro-Cia, M.; Rahmani, M.; Sidiropoulos, T. P.; Hong, M.; Oulton, R. F.; Maier, S. A. Multiresonant broadband optical antennas as efficient tunable nanosources of second harmonic light. *Nano letters* **2012**, *12*, 4997–5002.

(6) Zhang, Y.; Grady, N. K.; Ayala-Orozco, C.; Halas, N. J. Three-dimensional nanostructures as highly efficient generators of second harmonic light. *Nano letters* **2011**, *11*, 5519–5523.

(7) Capretti, A.; Walsh, G. F.; Minissale, S.; Trevino, J.; Forestiere, C.; Miano, G.; Dal Negro, L. Multipolar second harmonic generation from planar arrays of Au nanoparticles. *Optics express* **2012**, *20*, 15797–15806.

(8) Capretti, A.; Pecora, E. F.; Forestiere, C.; Dal Negro, L.; Miano, G. Size-dependent second-harmonic generation from gold nanoparticles. *Physical Review B* **2014**, *89*, 125414.

(9) Boyd, R. W. *Nonlinear optics*; Academic press, 2003.

(10) Zernike, F.; Midwinter, J. E. *Applied nonlinear optics*; Courier Corporation, 2006.

(11) Lee, J.; Tymchenko, M.; Argyropoulos, C.; Chen, P.-Y.; Lu, F.; Demmerle, F.; Boehm, G.; Amann, M.-C.; Alù, A.; Belkin, M. A. Giant nonlinear response from plasmonic metasurfaces coupled to intersubband transitions. *Nature* **2014**, *511*, 65–69.

(12)

(13) Cai, W.; Vasudev, A. P.; Brongersma, M. L. Electrically controlled nonlinear generation of light with plasmonics. *Science* **2011**, *333*, 1720–1723.

(14) Kang, L.; Cui, Y.; Lan, S.; Rodrigues, S. P.; Brongersma, M. L.; Cai, W. Electrifying photonic metamaterials for tunable nonlinear optics. *Nature communications* **2014**, *5*.

(15) Cornet, M.; Degert, J.; Abraham, E.; Freysz, E. Terahertz-field-induced second harmonic generation through Pockels effect in zinc telluride crystal. *Optics letters* **2014**, *39*, 5921–5924.

(16) Pestov, D.; Lozovoy, V. V.; Dantus, M. Multiple Independent Comb Shaping (MICS): Phase-only generation of optical pulse sequences. *Opt. Express* **2009**, *17*, 14351–14361.